JOURNAL OF MATERIALS SCIENCE 23 (1988) 1324–1328

Formation and properties of amorphous $(Fe_{1-x}Nb_x)_lB_{100-l}$

S. T. LIN, C. L. LEE
Department of Physics, National Cheng Kung University, Tainan, Taiwan

Amorphous $(Fe_{1-x}Nb_x)_lB_{100-l}$ alloys with $0 \leqslant x \leqslant 0.15$ and $74 \leqslant l \leqslant 86$ have been formed and their thermal stability, mechanical and magnetic properties have also been studied. Substitution of niobium for iron is found to increase the glass transition temperature T_g, crystallization temperature T_x, and microhardness H_v, but to decrease the magnetization σ and Curie temperature T_c. The effects of niobium on T_x, H_v, σ and T_c in iron-based amorphous alloys are similar to those of chromium, manganese, molybdenum, tungsten and vanadium.

1. Introduction

Amorphous $(Fe_{1-x}Nb_x)_lB_{100-l}$ alloys have been prepared by the melt-spinning technique and the effects of niobium on the formation ability, glass transition and crystallization temperatures, microhardness, magnetization and Curie temperature were studied.

2. Experimental procedures

The amorphous nature of the prepared samples was checked by X-ray diffraction. Glass transition and crystallization temperatures were determined by differential thermal analysis (DTA) with a heating rate $20°C\,min^{-1}$. Room-temperature magnetization was measured using a vibrating sample magnetometer (VSA) under a field of 10 kOe and the Curie temperature was determined from thermomagnetization curves, also measured using the VSA. Microhardness was measured using a Vickers indenter with a load of 100 g.

3. Results and discussion

3.1. Formation of amorphous Fe–Nb–B

$(Fe_{1-x}Nb_x)_lB_{100-l}$ samples formed as amorphous solids are within the range $0 \leqslant x \leqslant 0.15$, $74 \leqslant l \leqslant 86$, as shown in Fig. 1, where (+) denotes the samples which are brittle in the as-quenched state, but X-ray diffraction reveals they are still amorphous, while (○) denotes the samples which are ductile and amorphous.

3.2. Glass transition and crystallization temperatures

The glass transition temperature T_g and crystallization temperature T_x are defined in Fig. 2. T_g and T_{x1} (first peak crystallization temperature) as a function of x for a fixed value of l are shown in Figs 3 and 4, respectively. Glass transition temperatures of Fe_lB_{100-l} alloys not containing niobium cannot be detected by DTA measurements. Thus, their T_g values were inferred to be embedded in crystallization peaks. As displayed in Figs 3 and 4, for a fixed l, increasing x (i.e. increasing the concentration ratio C_{Nb}/C_{Fe}) increases T_g and T_{x1}, while for a fixed x, T_g and T_{x1} increase with decreasing l (i.e. increasing boron concentration, C_B). Table I lists the crystallization peak numbers and peak temperatures of the amorphous series $(Fe_{1-x}B_x)_l B_{100-l}$ as a function of x and l. It is seen that for Fe_lB_{100-l} alloys there are two crystallization peaks for $l \geqslant 84$ and one for $l \leqslant 82$. This is in agreement with the previous results reported [1, 2]; increasing x not only enhances the crystallization peak numbers, but also increases all the crystallization peak temperatures.

Table II lists the values of the difference between T_{x1} and T_g. $(T_{x1} - T_g)$ is obviously seen to increase with increasing x. Coleman [3] showed for an amorphous series of Fe–Ni–P–B alloys that the larger the value of $(T_{x1} - T_g)$, the larger the activation energy for crystal-

TABLE I Crystallization peak numbers and peak temperatures of amorphous $(Fe_{1-x}Nb_x)_{100-l}B_l$

x	Peak temperature (°C)							
	$l = 86$	$l = 84$	$l = 82$	$l = 80$	$l = 78$	$l = 76$	$l = 75$	$l = 74$
0.00	396	418	466	463	470	479	480	481
	497	495						
0.05	438	501	524	540	560	580		594
	556	610	606					
	659	660						
0.10	483	550	570	587	600	617		648
	617	644	662	750	759	786		837
	670	772						
0.15		603	632	624	634	647		
		722	750	750	761	785		
		831	835	830				

0022–2461/88 $03.00 + .12

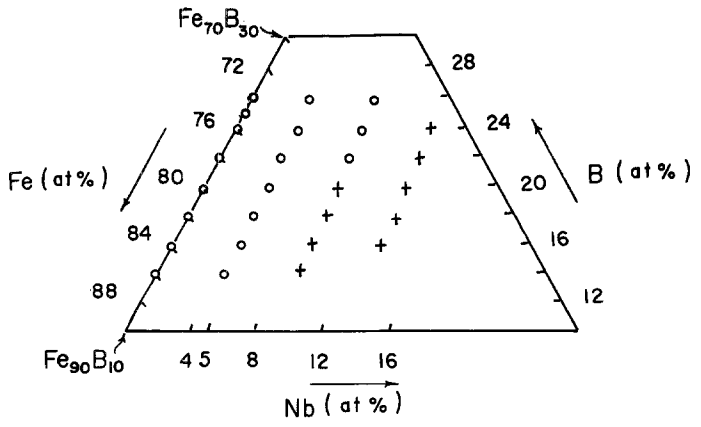

Figure 1 Composition range for formation of amorphous phase in Fe–Nb–B system: (+) brittle, (○) ductile.

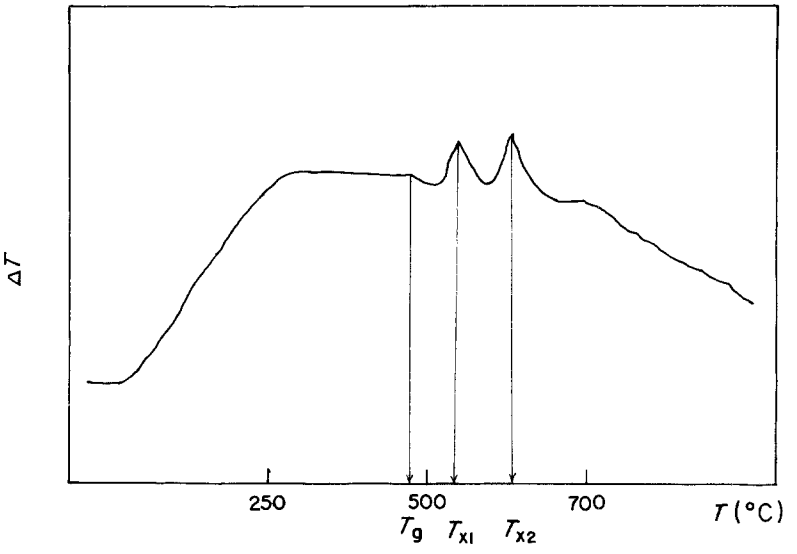

Figure 2 DTA trace of amorphous $(Fe_{0.95}Nb_{0.05})_{82}B_{18}$.

lization. If this is universally true in amorphous alloys, then our results show that substitution of iron by niobium greatly increases the thermal stability against crystallization.

3.3. Magnetization and Curie temperature

The room-temperature magnetization σ and Curie temperature T_c plotted against I for a fixed x are presented in Figs 5 and 6, respectively. For a fixed I, both σ and T_c decrease with increasing $x = C_{Nb}/C_{Fe}$, while for a fixed x except for $x = 0$, both σ and T_c decrease monotonically with increasing I (i.e. decreasing C_B). Since a niobium atom has a much larger atomic radius than an iron atom, the rapid drop in T_c for iron replacement by niobium may be attributed to the change in iron coordination number and the distance between iron atoms.

3.4. Hardness

Fig. 7 displays the microhardness H_v against I for a fixed x. H_v is seen to increase with increasing both C_{Nb}/C_{Fe} and C_B. With iron substituted by niobium, a microhardness as high as $1285\,kg\,mm^{-2}$ for $(Fe_{0.9}Nb_{0.1})_{74}B_{26}$ was obtained.

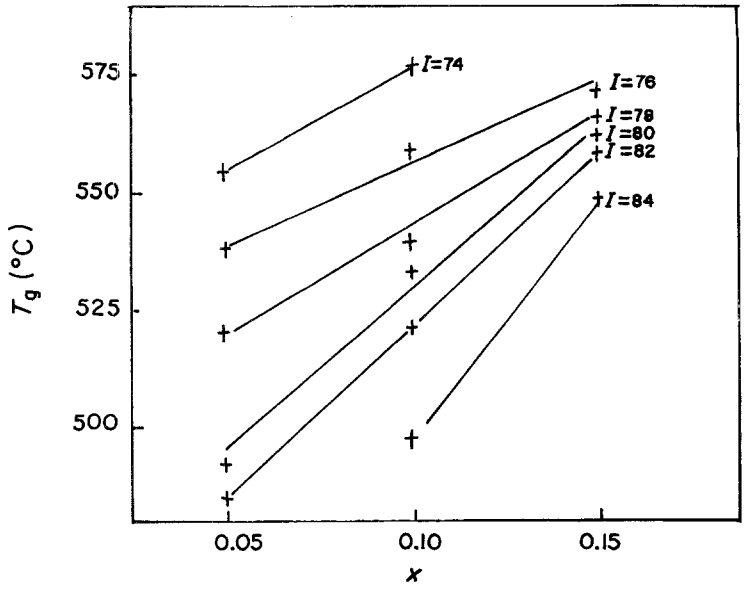

Figure 3 Glass transition temperature T_g of amorphous $(Fe_{1-x}Nb_x)_{100-I}B_I$ as a function of x.

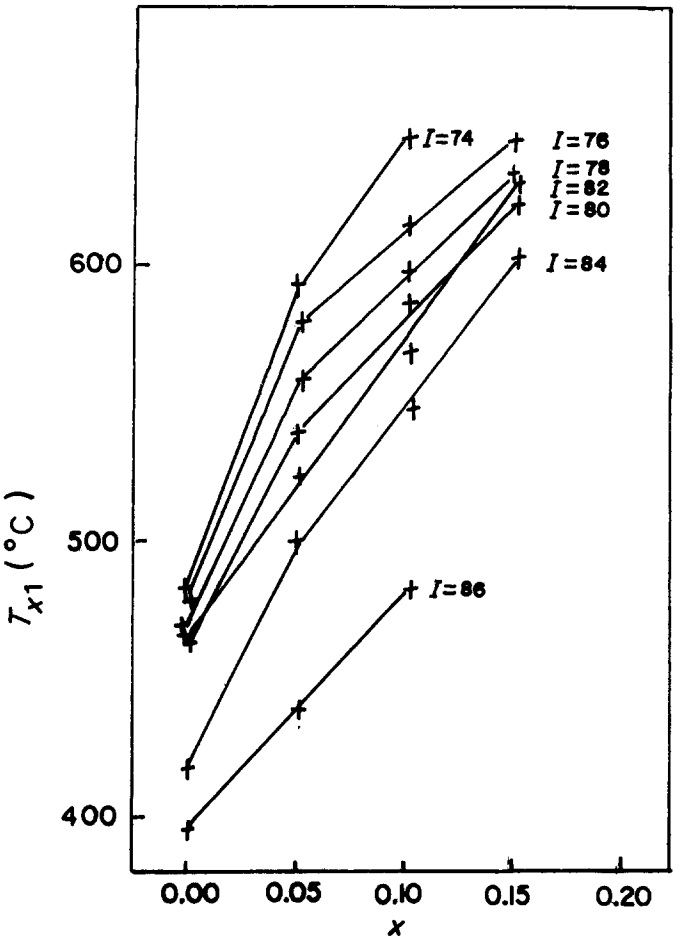

Figure 4 First peak crystallization temperature T_{x1} of $(Fe_{1-x}Nb_x)_{100-I}B_I$ as a function of x.

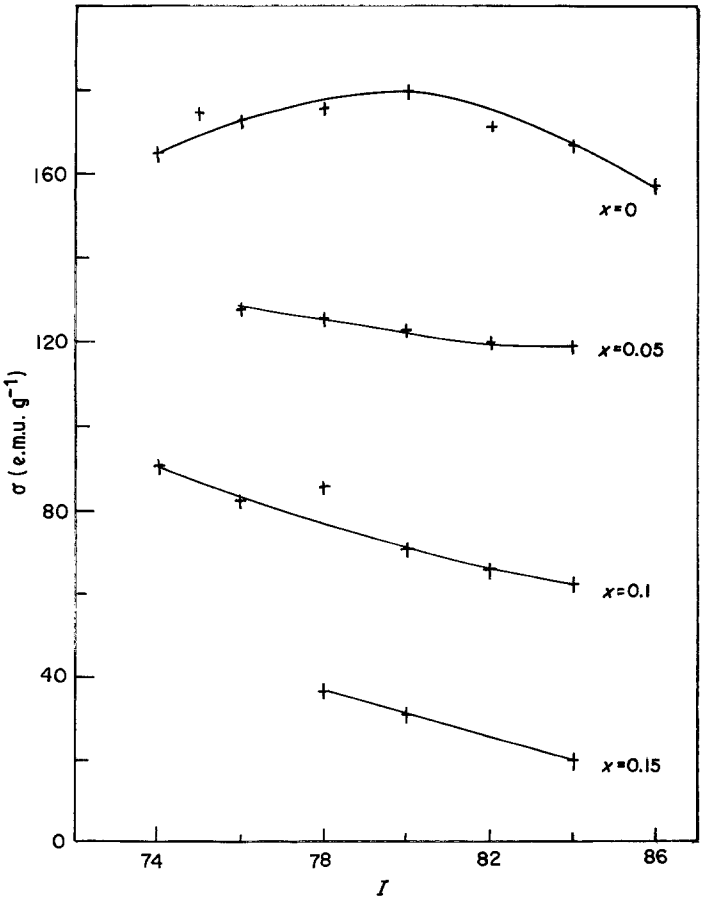

Figure 5 Room-temperature magnetization σ of $(Fe_{1-x}Nb_x)_{100-I}B_I$ as a function of I.

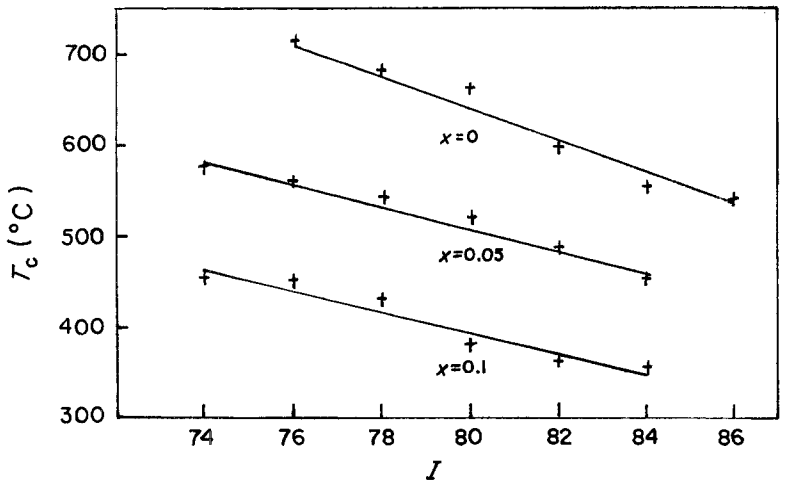

Figure 6 Curie temperature T_c of $(Fe_{1-x}Nb_x)_{100-I}B_I$ as a function of I.

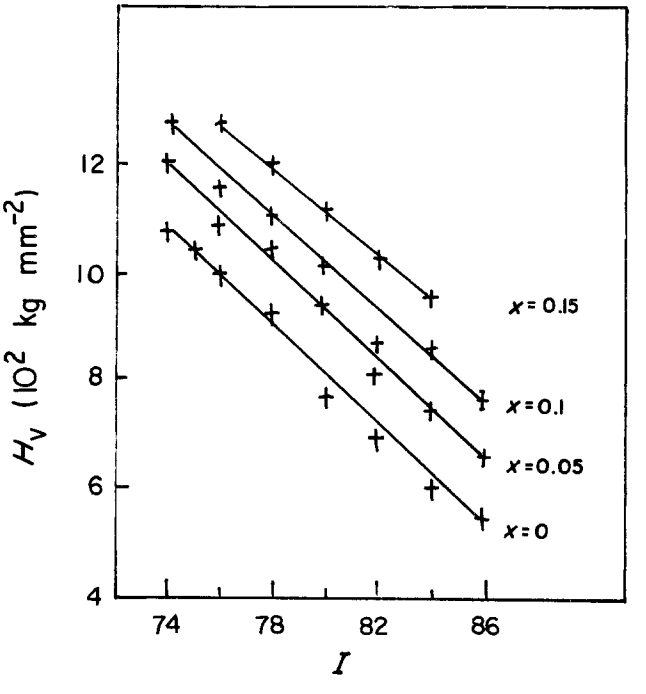

Figure 7 Microhardness H_v of $(Fe_{1-x}Nb_x)_{100-I}B_I$ as a function of I.

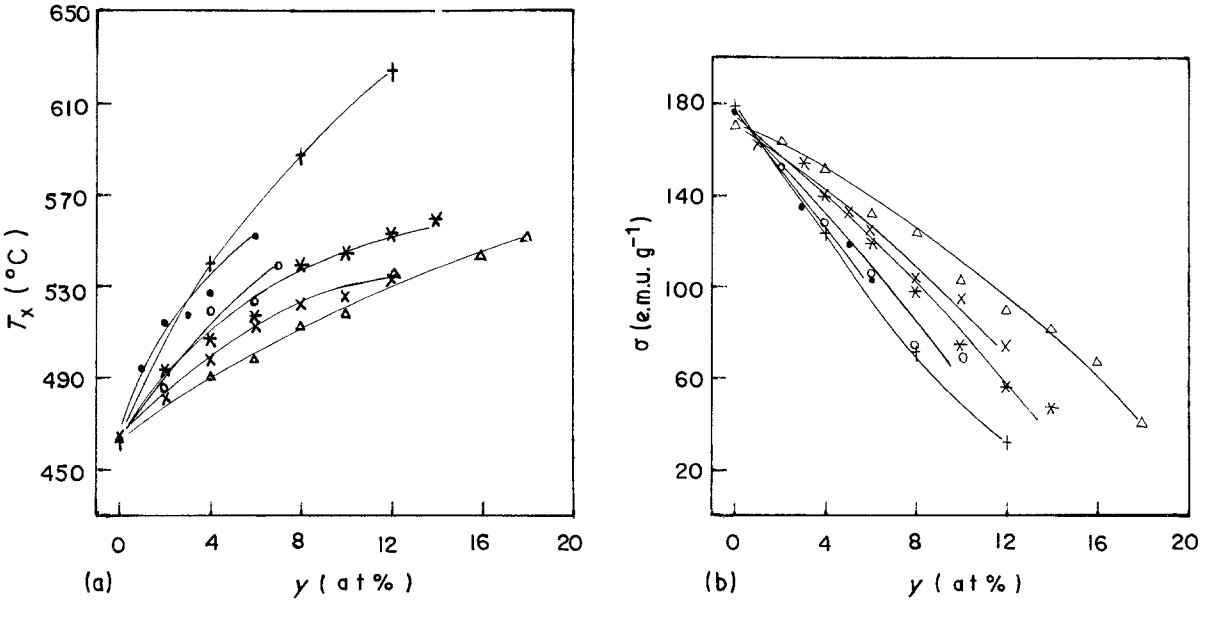

Figure 8 Comparisons of (a) T_x, (b) σ, (c) T_c and (d) H_v for $Fe_{80-y}Nb_yB_{20}$ with those of Fe_{80-y}-(Cr, Mn, Mo, W, V)$_yB_{14}Si_6$. (+) Nb, (*) Cr, (△) Mn, (○) Mo, (●) W, (x) V.

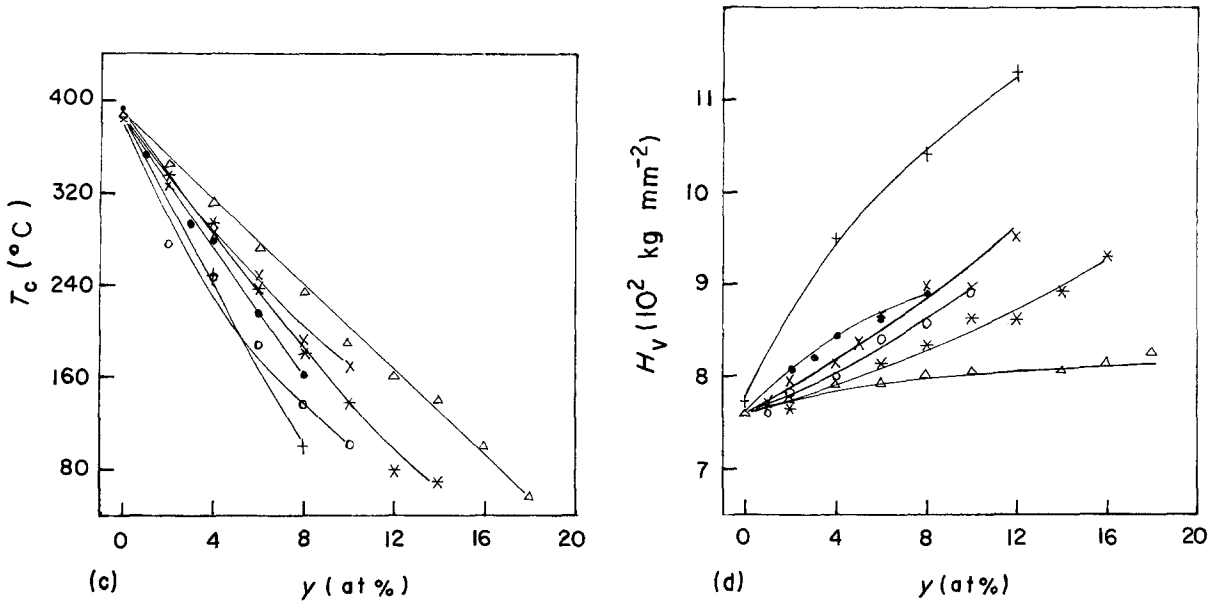

Figure 8 Continued.

3.5. Comparisons of T_x, σ, T_c and H_v of amorphous $Fe_{80-y}Nb_yB_{20}$ with those of amorphous Fe_{80-y}–(Cr, Mn, Mo, W, V)$_yB_{14}Si_6$ [4]

Figs 8a to d, show T_x, σ, T_c, and H_v, respectively, against y. These figures indicate that the effects of niobium and chromium, manganese, molybdenum, tungsten and vanadium on T_x, σ, T_c and H_v have the same trend, i.e. addition of these elements to iron-based amorphous alloys increases H_v and T_x, but decreases T_c and σ. However, how these elements affect these physical properties is still not quite understood and deserves further theoretical and experimental studies.

TABLE II Values of $(T_{x1} - T_g)$ for $(Fe_{1-x}Nb_x)_{100-I}B_I$

x	$(T_{x1} - T_g)$ (°C)					
	$I = 84$	$I = 82$	$I = 80$	$I = 78$	$I = 76$	$I = 74$
0.05	–	39	48	39	41	39
0.10	52	48	53	60	58	71
0.15	54	74	61	68	75	–

Acknowledgement

We are indebted to the National Science Council of the Republic of China for the financial support of this work.

References

1. J. L. WALTER, S. F. BARTRAM and R. R. RUSSELL, *Metall. Trans* **9A** (1978) 803.
2. J. L. WALTER, S. F. BARTRAM and I. MELLA, *Sci. Eng.* **36** (1978) 193.
3. E. COLEMAN, *Mater. Sci. Eng.* **23** (1976) 161.
4. S. T. LIN, H. B. WU and W. T. KU, unpublished work.

Received 11 May
and accepted 17 August 1987